ESD-TR-87-084

Project Report
ODT-8

Distortion of Wideband Carbon Dioxide Laser Radar Waveforms due to Atmospheric Dispersion and Absorption

R.E. Knowlden
A.L. Kachelmyer
W.E. Keicher

12 November 1987

Lincoln Laboratory
MASSACHUSETTS INSTITUTE OF TECHNOLOGY
LEXINGTON, MASSACHUSETTS

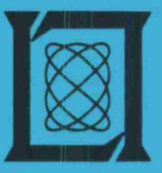

**Prepared for the Defense Advanced Research Projects Agency
under Electronic Systems Division Contract F19628-85-C-0002.**

The work reported in this document was performed at Lincoln Laboratory, a center for research operated by Massachusetts Institute of Technology. This work was sponsored by the Defense Advanced Research Projects Agency under Air Force Contract F19628-85-C-0002 (ARPA Order 3391).

This technical report has been reviewed and is approved for publication.

FOR THE COMMANDER

Hugh L. Southall, Lt. Col., USAF
Chief, ESD Lincoln Laboratory Project Office

MASSACHUSETTS INSTITUTE OF TECHNOLOGY
LINCOLN LABORATORY

DISTORTION OF WIDEBAND CARBON DIOXIDE LASER RADAR WAVEFORMS DUE TO ATMOSPHERIC DISPERSION AND ABSORPTION

R.E. KNOWLDEN
A.L. KACHELMYER
W.E. KEICHER
Group 52

PROJECT REPORT ODT-8

12 NOVEMBER 1987

LEXINGTON MASSACHUSETTS

ABSTRACT

Atmospheric dispersion is shown to have a significant effect on wideband coherent laser radars operating on a transition of ordinary carbon dioxide (CO_2). Calculations are performed for a hypothetical ground-based laser radar that is observing targets in low Earth orbit. Linear frequency modulated (LFM) waveforms of bandwidths 200 MHz, 500 MHz, 1 GHz, and 2 GHz are used. The use of a laser radar operating with a different carbon isotope ($^{13}C^{16}O_2$) is suggested to avoid the dispersion problem, and also to reduce the atmospheric absorption.

TABLE OF CONTENTS

LIST OF ILLUSTRATIONS

1. INTRODUCTION

Carbon dioxide (CO_2) lasers can be used in coherent optical radars. Some CO_2 radars will operate through the Earth's atmosphere.

Atmospheric CO_2 and other gases will absorb the laser radiation. Because this is resonant absorption, dispersion will also occur. The combined effects of absorption and dispersion can significantly degrade the resolution of the radar. These effects are calculated in this paper. The particular example chosen for calculation is for a radar that is used to determine the precise range to a satellite in Earth orbit. This example was chosen to show the effects of CO_2 absorption both at low and high altitudes in the atmosphere.

2. METHOD OF CALCULATION

The following discussion describes the method used to estimate the atmospheric absorption and dispersion effects. Some of the approximations employed are discussed.

The Air Force Geophysics Laboratory's code for computing atmospheric spectral transmittance with high resolution (FASCOD2[1]), with its extensive compilation of spectral data, is a convenient tool for calculating atmospheric absorption. In principle, the code could be modified to integrate optical path length as well as absorption through the atmosphere; an approach similar to this was employed by Halliday[2] to estimate the dispersion effects.

Alternately, the Kramers-Kronig relations[3] can be used to estimate the dispersion from a calculation of only the absorption. This method was selected because of its ease of use. The basic form of the relation used is:

$$\chi'(\omega) = \frac{1}{\pi} P.V. \int_{-\infty}^{\infty} d\omega' \frac{\chi''(\omega')}{\omega' - \omega} \tag{1}$$

where χ' is the real part of the medium's complex susceptibility ($\chi = \chi' + j\chi''$) as a function of angular frequency ω, and χ'' is the imaginary part. (P. V.) indicates Cauchy principal value. If n_c is the complex refractive index of the medium ($n_c = n + jk$),

$$n_c^2 = 1 + 4\pi\chi \tag{2}$$

but for the atmosphere

$$| n_c - 1 | << 1 \tag{3}$$

so that

$$n_c - 1 \approx 2\pi \chi \tag{4}$$

The relation between the absorption coefficient (α) and the imaginary part (k) of a medium's complex index (n_c) is

$$\alpha = 4\pi \nu k \tag{5}$$

where ν is the frequency (wavenumber) of the radiation ($\omega = 2\pi \nu$). For a large absorption coefficient of 1 cm^{-1}, and for $\nu = 1000\ cm^{-1}$ (wavelength 10 μm), $k \approx 8 \times 10^{-5}$. A more typical absorption coefficient in the atmosphere would be of order 1 km^{-1}, or $1 \times 10^{-5}\ cm^{-1}$. Under the approximation in Equation 3, Equation 1 may be rewritten as

$$n(\nu) - 1 \approx \frac{1}{\pi} P.V. \int_{-\infty}^{\infty} d\nu' \frac{k(\nu')}{\nu' - \nu} \tag{6}$$

Define a function $\kappa(\nu)$

$$\kappa(\nu) = \int_p ds\ k(\nu) \tag{7}$$

(defined as a line integral along path p, which may be curved in the atmosphere due to refraction) and another as

$$\eta(\nu) = \int_p ds\ [n(\nu) - 1] \tag{8}$$

then η may be expressed in terms of κ by

$$\eta(\nu) \approx \frac{1}{\pi} P.V. \int_{-\infty}^{\infty} d\nu' \frac{\kappa(\nu')}{\nu' - \nu} \tag{9}$$

The function $\kappa(\nu)$ is obtained from the FASCOD2 output. In practice, the range in ν must be finite, but a suitably large interval may be chosen to obtain a good estimate of the effect of the atmospheric dispersion near a spectral feature.

Fourier methods may conveniently be used to evaluate Equation 9. If the Fourier transform of $\kappa(\nu)$ is defined

$$K(x) = \int_{-\infty}^{\infty} d\nu \; e^{-j2\pi x \nu} \kappa(\nu) \tag{10}$$

and the Fourier transform of $\eta(\nu)$ is similarly defined to be $H(x)$, then Equation 9 can be expressed in the transform domain (c.f. Bracewell [4]) as

$$H(x) = \frac{j}{2} \, \mathrm{sgn}(x) \, K(x) \tag{11}$$

where the signum function is defined

$$\mathrm{sgn}(x) = \begin{cases} -1 ; & x < 0 \\ 0 ; & x = 0 \\ 1 ; & x > 0 \end{cases} \tag{12}$$

The Fourier transforms are performed in practice using a fast Fourier transform (FFT). Some care is required to minimize the effects of the finite interval of the calculation.

As a test case, a Lorentzian line shape is used for k and the dispersion curve ($n-1$) is computed using the above method and compared to the true values. The functions for k and ($n-1$) are

$$k(\nu) = \frac{k_0 \left(\frac{\gamma^2}{4}\right)}{\left[(\nu - \nu_0)^2 + \left(\frac{\gamma^2}{4}\right) \right]} \tag{13}$$

and

$$n(\nu) - 1 = \frac{-k_0 (\nu - \nu_0)(\frac{\gamma}{2})}{[(\nu - \nu_0)^2 + (\frac{\gamma^2}{4})]} \qquad (14)$$

where k_0 is the on-resonance value of k, γ is the half width half strength frequency for the line, and ν_0 is the line center frequency. For $k_0 = 1 = \gamma$, and $\nu_0 = 0$, Figure 1 shows the values for k and (n-1). To test the validity of the approximation to the Kramers - Kronig calculation, the values from Equation 13 were used in a calculation and compared to the analytical result in Equation 14. Figure 2 shows the arithmetic difference between the function from Equation 14 and the approximation. For the Kramers-Kronig calculation, the spectral width of the calculation was 100 full widths (200 γ) over 1024 points, with an additional 1024 points appended to make the number of elements in the fast Fourier transform equal 2048 points. The error relative to the analytical result is neglible here, because phase errors of less than 2 mrad peak - to - peak cannot significantly increase the range sidelobes or broaden the main lobe.

3. KRAMERS-KRONIG CALCULATIONS FROM FASCOD2 DATA

Figure 3 shows the optical depth of the atmospheric absorption [$4\pi \nu \kappa(\nu)$] for a path to space as calculated using the FASCOD2 program. The path was from sea level, for the mid-latitude summer model, at a zenith angle of 45°. The strong absorption feature is that of the I P(22) line of atmospheric CO_2 at 942.3833 cm^{-1} (c.f. Bradley et al [5]). The FASCOD2 calculation has been compared with measured data from Kitt Peak[6] and found to give a good estimate of the CO_2 absorption. Figure 4 shows the results of a similar calculation but with the path from a 10 km altitude to space. The 10 km altitude represents a hypothetical case where the radar would operate from an aircraft to reduce the atmospheric absorption. Figure 3 shows pressure broadening of the CO_2 line at low altitudes, plus some broadband absorption that is due to water vapor.

The effects of the finite spectral interval in the absorption are minimized by extending the spectrum with dummy values. Figure 5 shows the spectrum of Figure 3, divided by the frequency (ν) and padded with the values from the ends of the FASCOD calculations. Note that the FFT will treat the interval as one cycle of a periodic spectrum, so the left side padding wraps over to the right of the interval. The padding also extends the number of points to a power of 2 for most efficient use of the FFT algorithm.

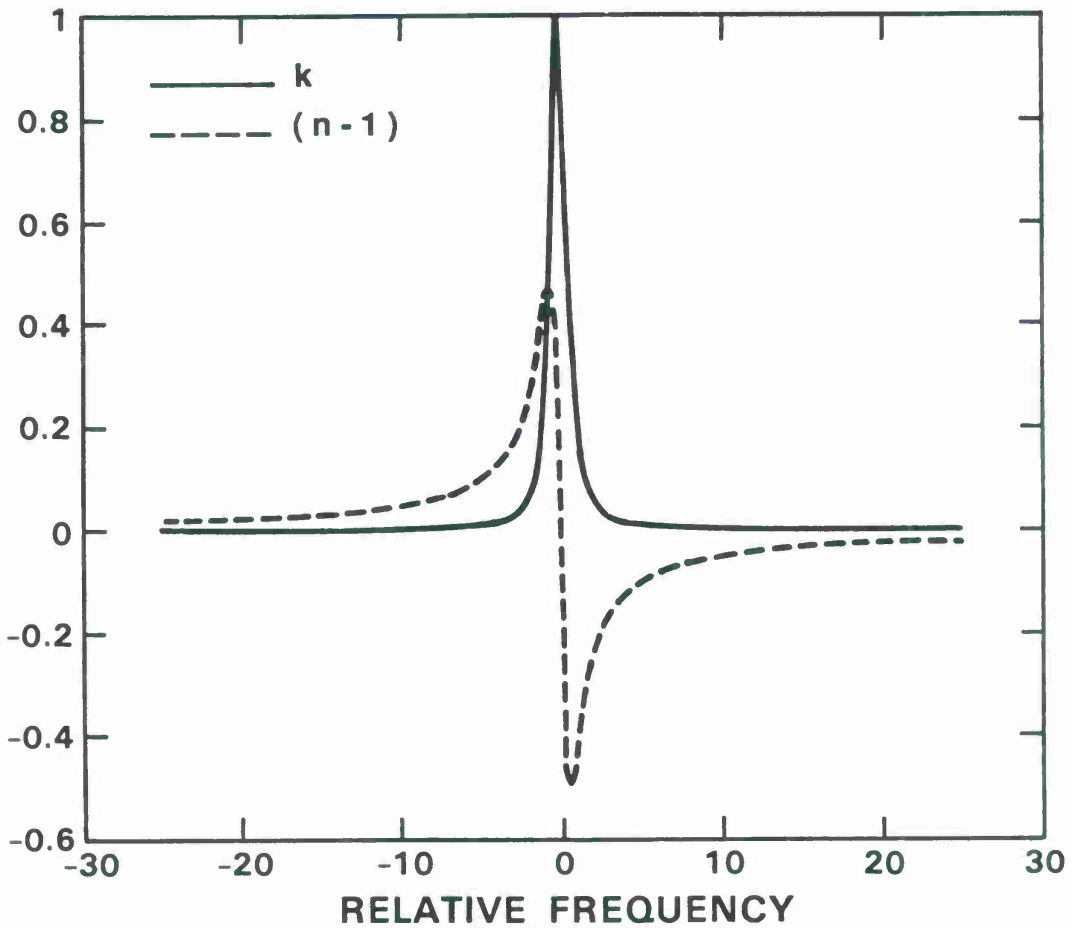

80197-3

Figure 1. k and (n-1) for a Lorentzian line.

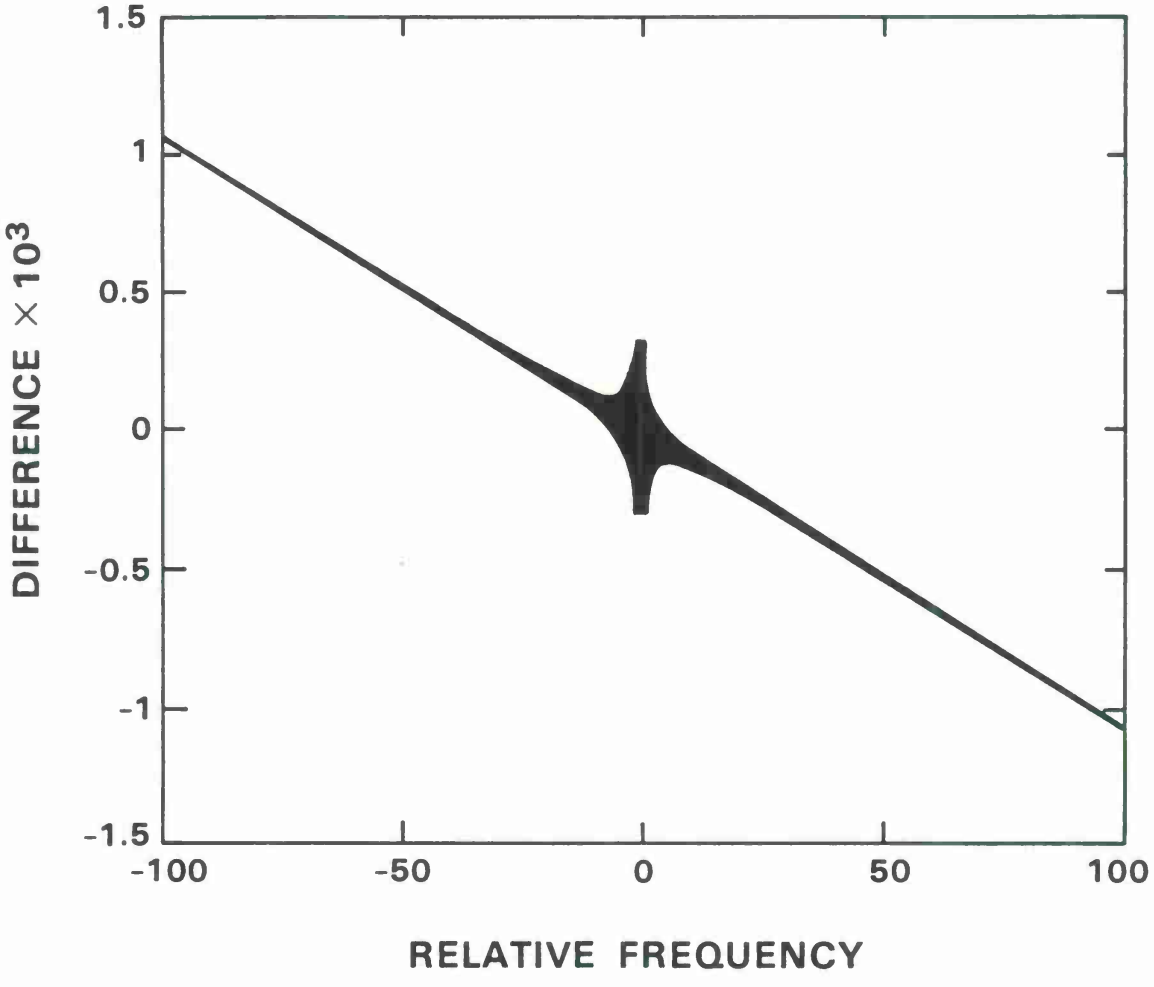

80197-4

Figure 2. Difference between (n-1) for a Lorentzian line and an approximate Kramers-Kronig calculation from k.

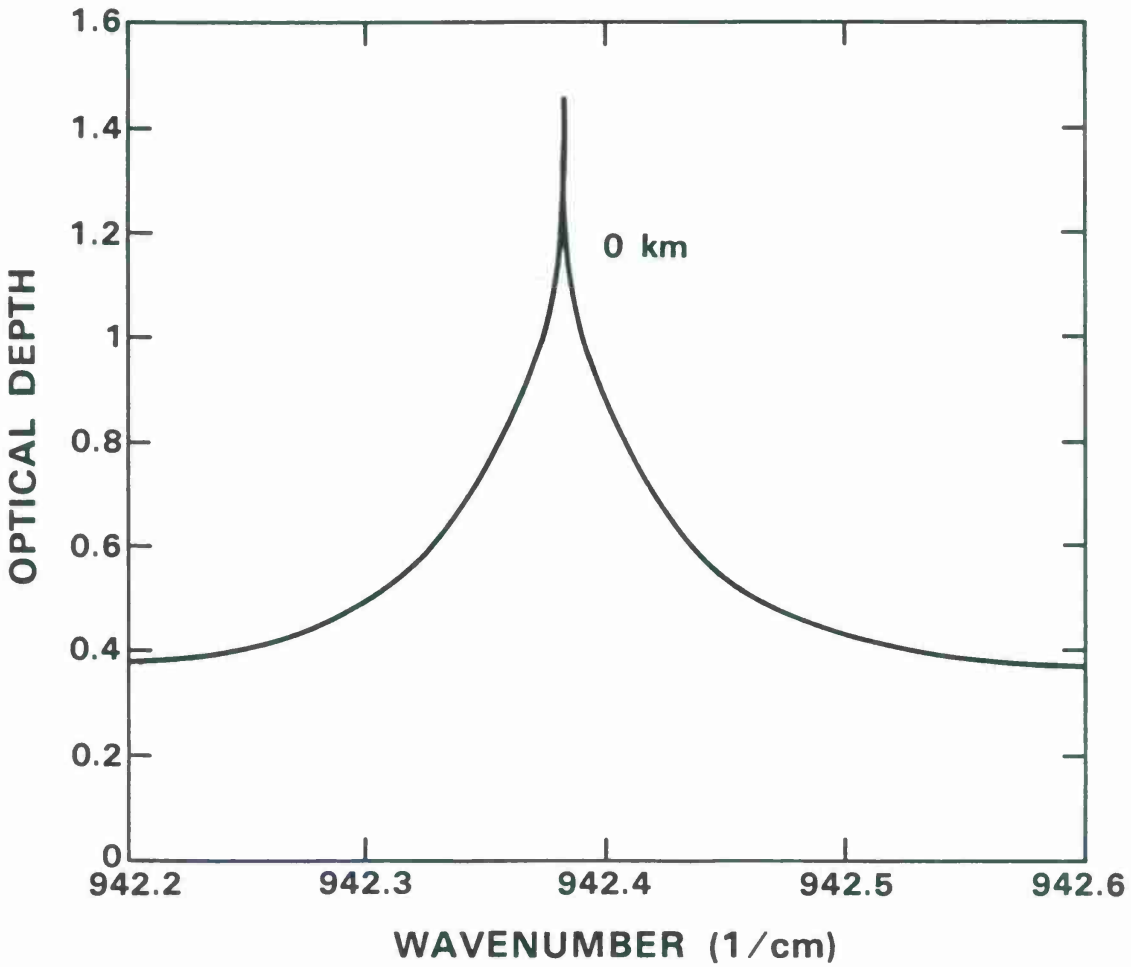

80197-5

Figure 3. Optical depth of the atmosphere computed using FASCOD2 for a path to space from sea level at a 45° zenith angle.

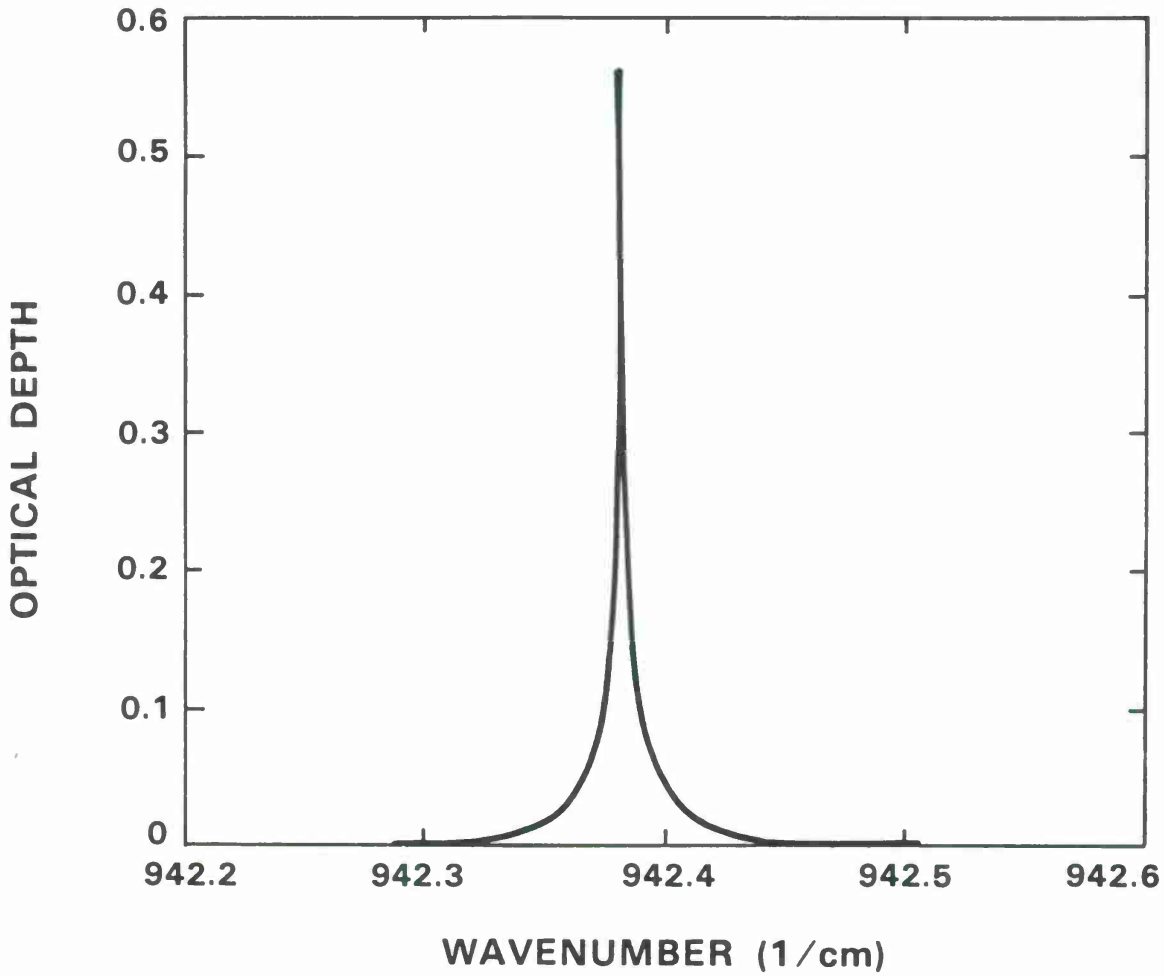

Figure 4. Atmospheric optical depth calculation from a 10 km altitude to space.

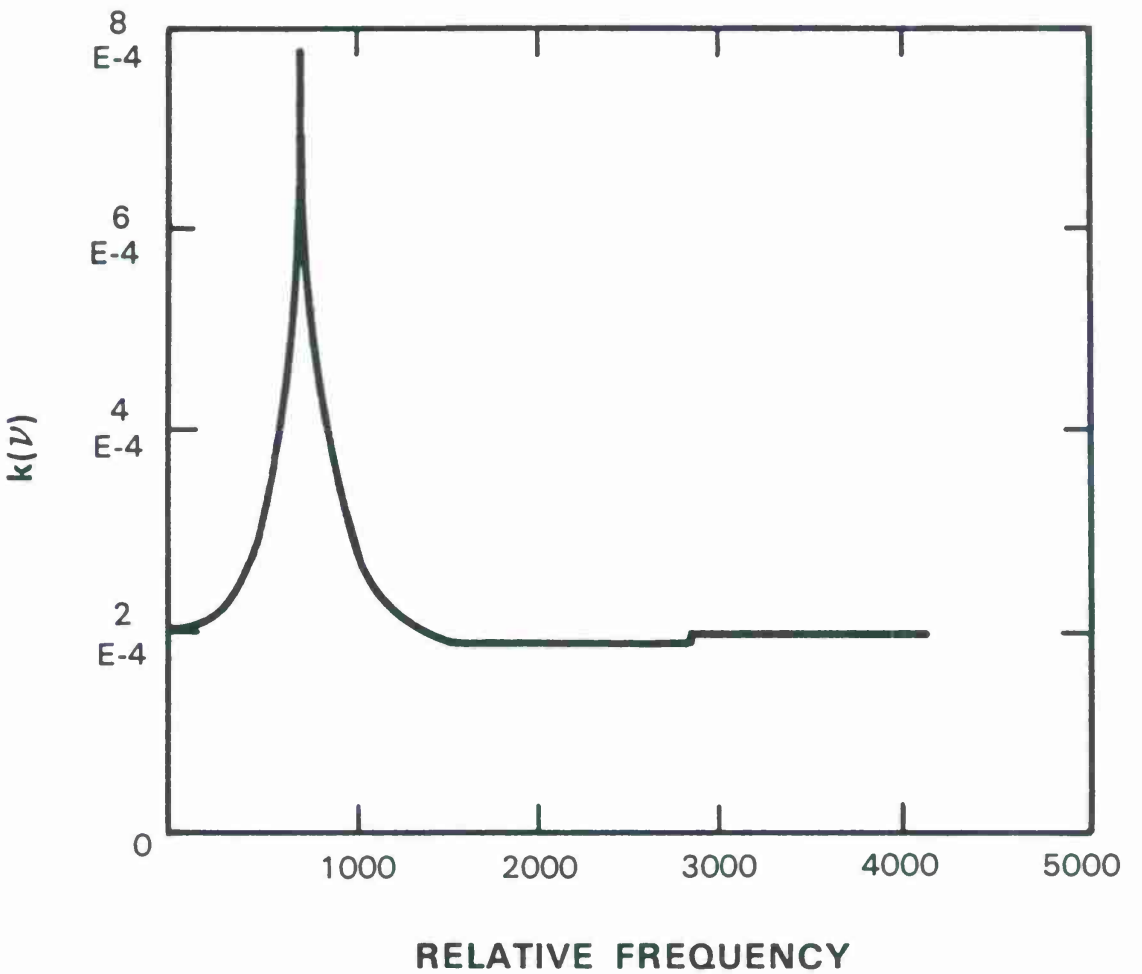

87854-1

Figure 5. Optical depth from sea level, with padding.

Padding the spectral interval gives the approximate Kramers-Kronig result shown in Figure 6. The disturbance caused by the discontinuity in the padded spectrum is set to be as far as possible from the center of the spectral data to minimize the errors it introduces. Most of the small residual error will be in the form of a linear phase error, corresponding to a small time shift. The computed phase function is then taken only over the spectral interval of the FASCOD data. Figure 7 is the result for the optical depth shown in Figure 3.

Figure 8 shows the optical path difference curves [$2\pi\,\nu\,\eta(\nu)$] computed with the optical depth in Figure 4.

Given the function $\kappa(\nu)$ and the dispersion $\eta(\nu)$, the transmittance transfer function is defined

$$T(\nu) = e^{j2\pi\nu[\eta(\nu)+j\kappa(\nu)]} \tag{15}$$

Figure 9 shows the amplitude and phase of the transfer function computed from the data in Figures 3 and 7. The zero frequency point is taken to be the CO_2 line center. This is for a single pass through the atmosphere. For an object in Earth orbit (Figure 10), the transfer function for the return path of a radar pulse will be displaced by the Doppler shift from the target, which can be as large as 1.5 GHz for 10 μm radiation. Figures 11 and 12 show the amplitude and phase of the two-way transfer functions (referred to the center frequency in the target return) for a 1.0 GHz Doppler shift with the atmospheres used in Figures 3 and 4. The 1 GHz shift from the target is sufficient so that the transfer function will be dominated by the upward path for laser waveform bandwidths much less than 2 GHz.

4. LINEAR FREQUENCY MODULATION

The type of waveform employed for the calculations uses linear frequency modulation (LFM) to obtain range resolution. The waveform is known as a *chirp* . In the complex notation, a single chirp is represented as

$$u_{LFM}(t) = a(t)\; e^{j2\pi[\nu_0 t + \frac{1}{2}(\frac{B}{\Delta t})t^2]} \tag{16}$$

where ν_0 is the carrier frequency ($\approx 3 \times 10^{13}$ Hz), B is the chirp bandwidth, and Δt is the chirp duration. For the simplest case,

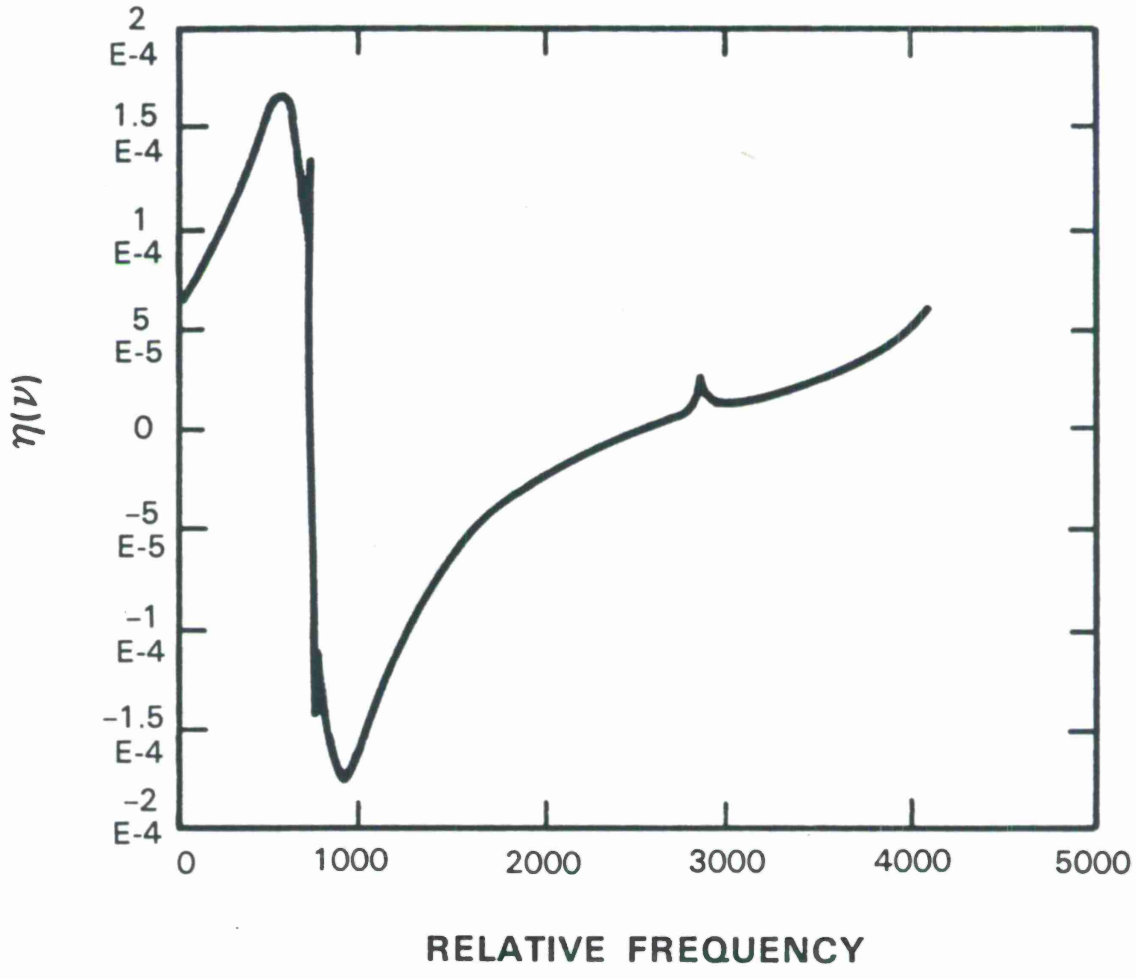

87854-2

Figure 6. Padded optical path difference computed by the Kramers-Kronig method for a path from sea level.

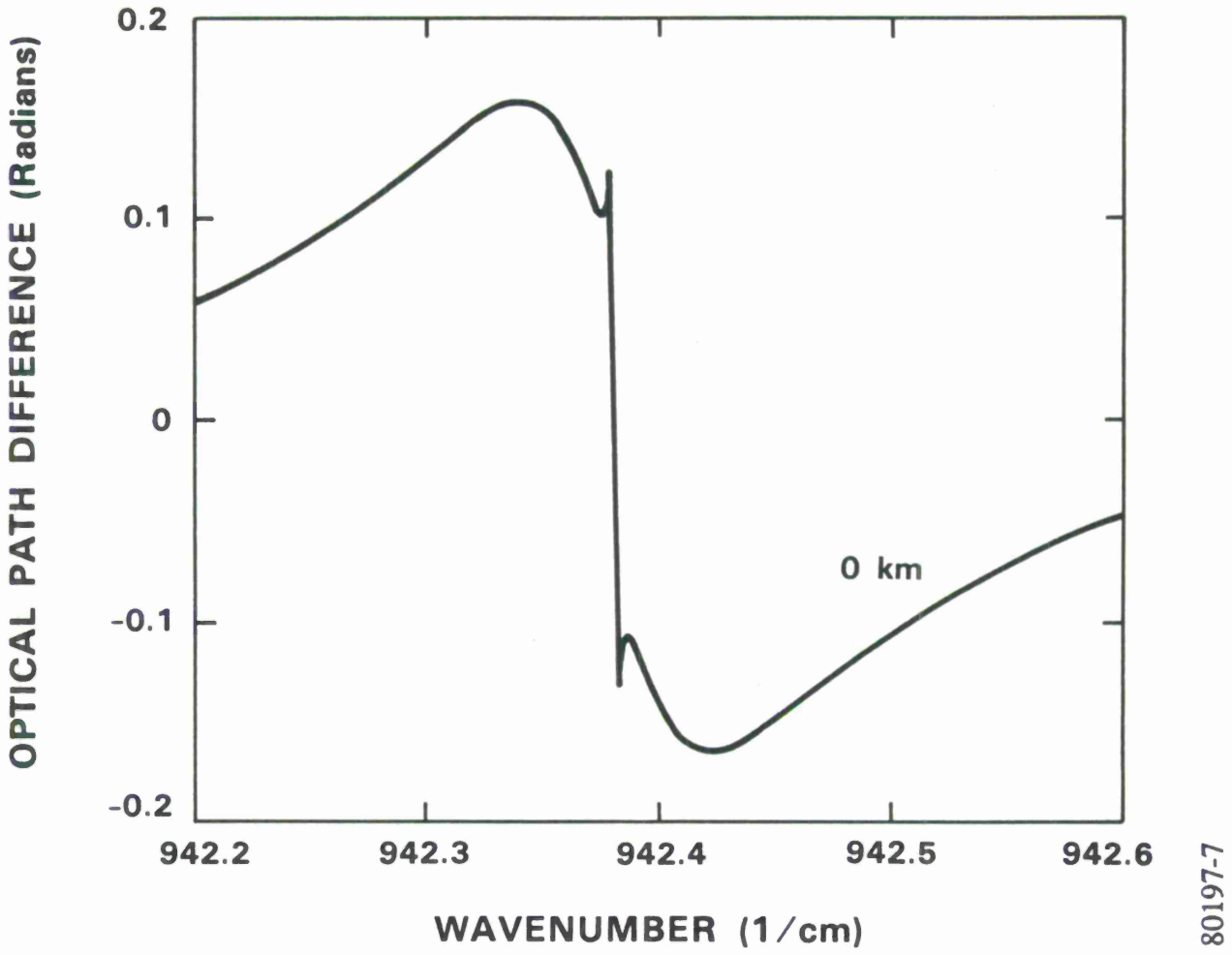

Figure 7. Optical path difference from sea level.

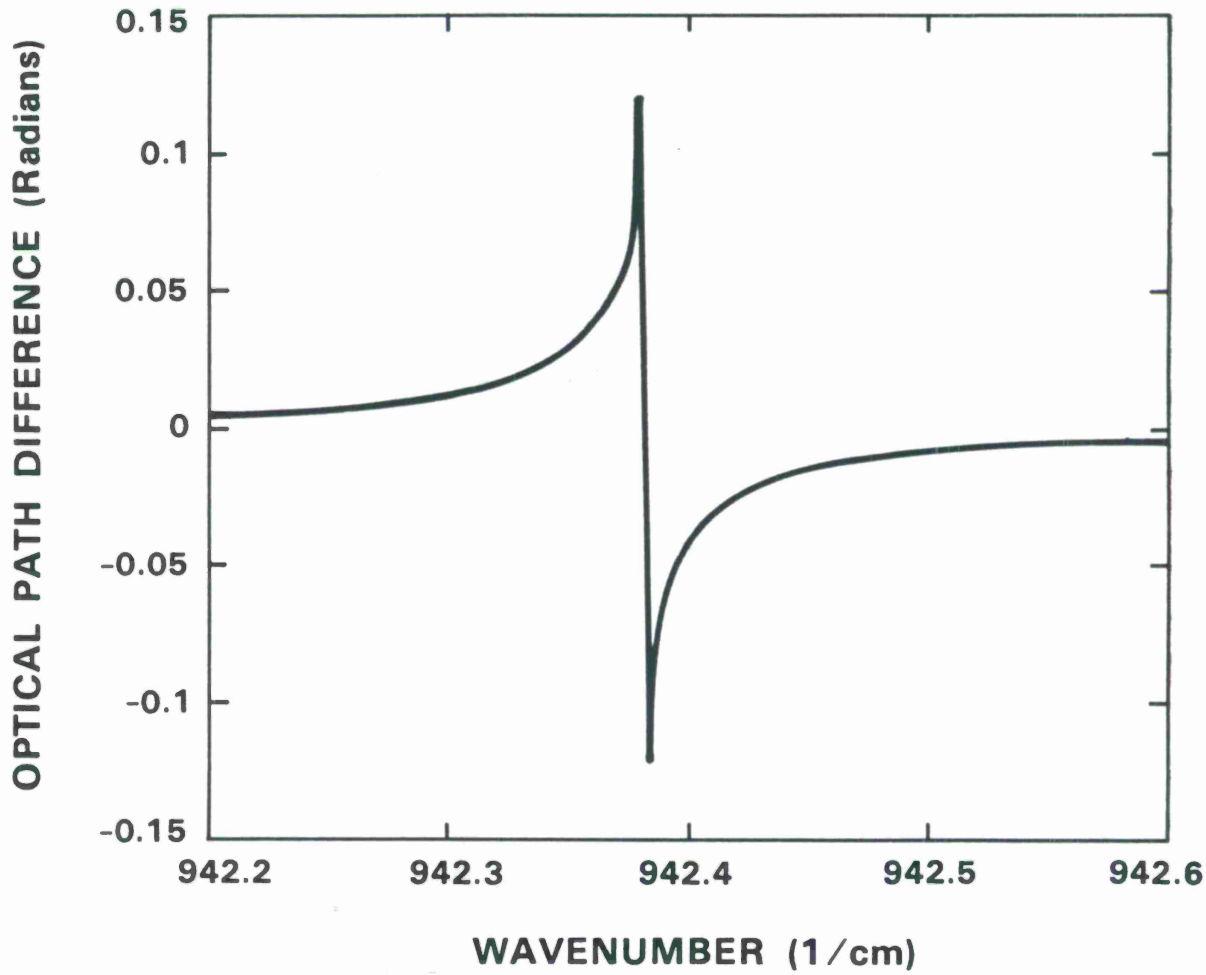

80197-8

Figure 8. Optical path difference for the path from 10 km.

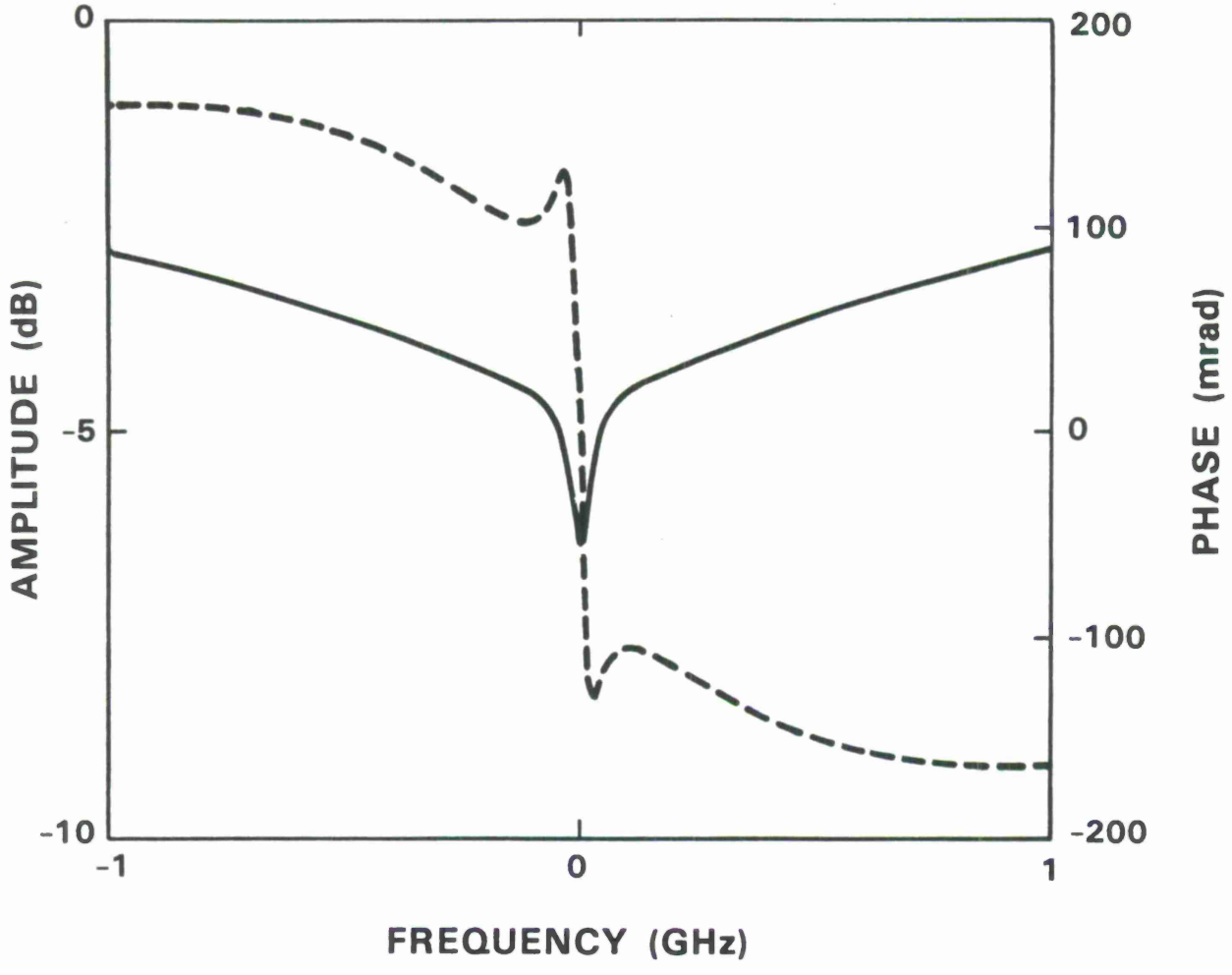

Figure 9. One-way atmospheric transfer function from sea level.

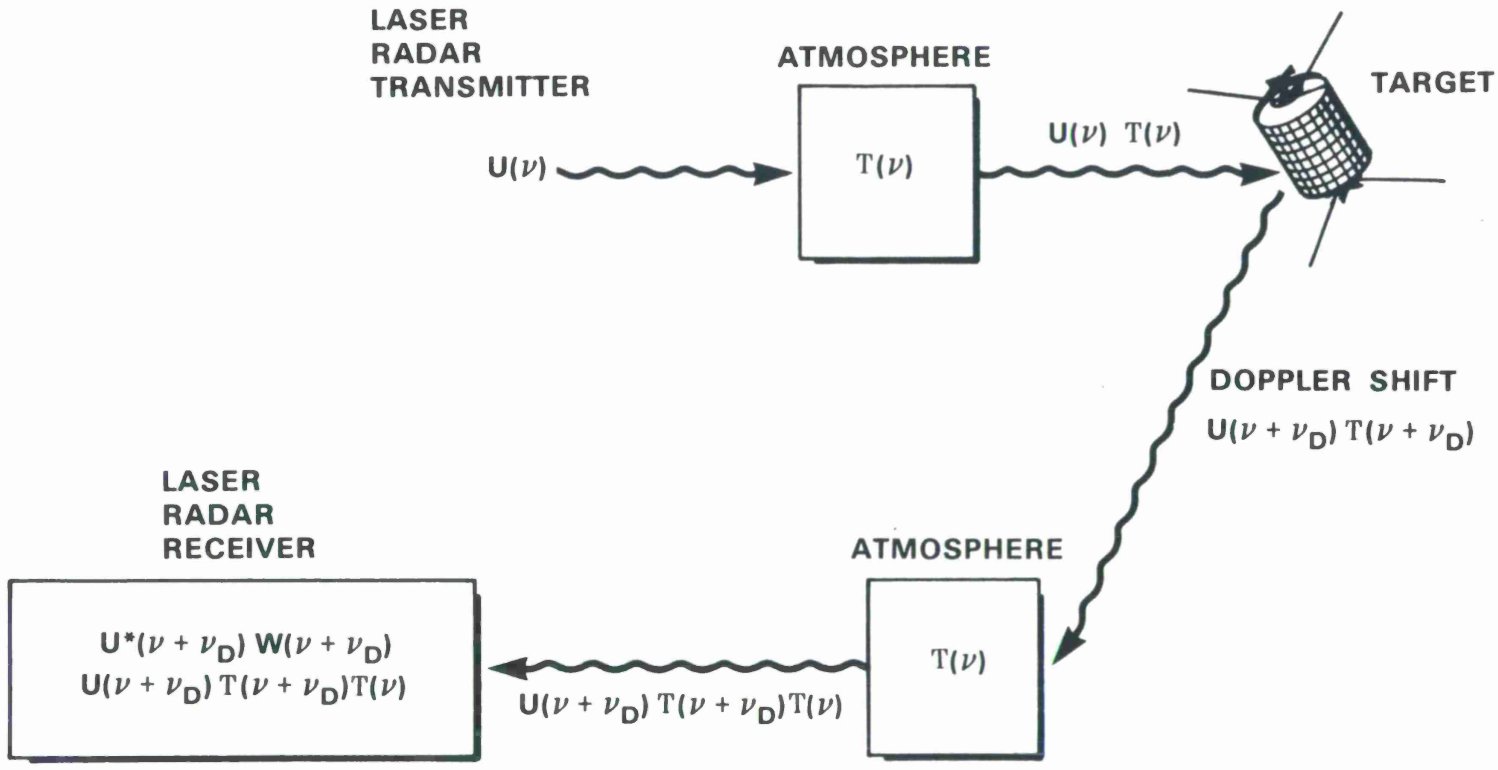

Figure 10. Illustration of the effects of target motion for a satellite in Earth orbit.

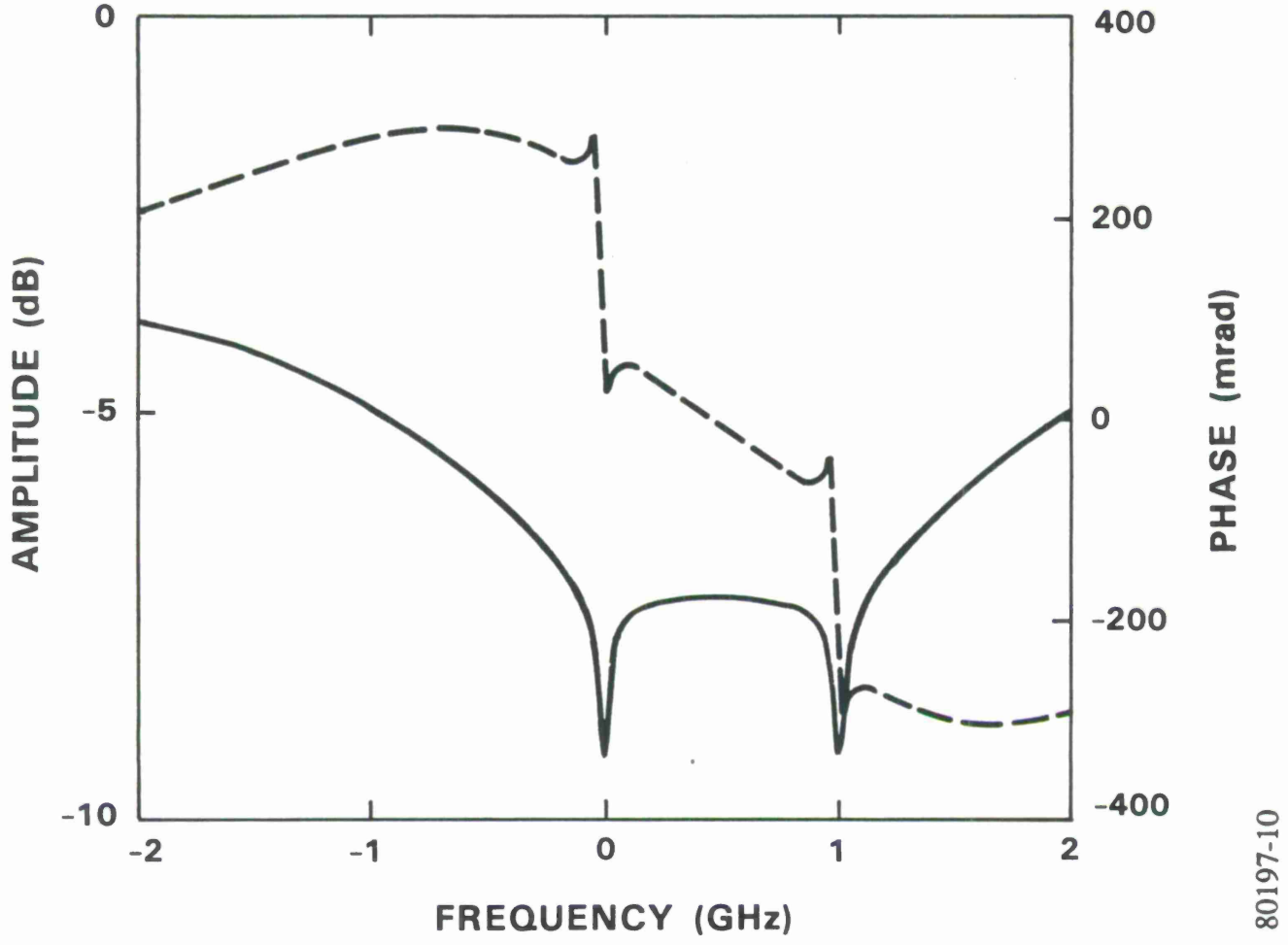

Figure 11. Transfer function for a two-way calculation from sea level, for a 1 GHz target Doppler shift.

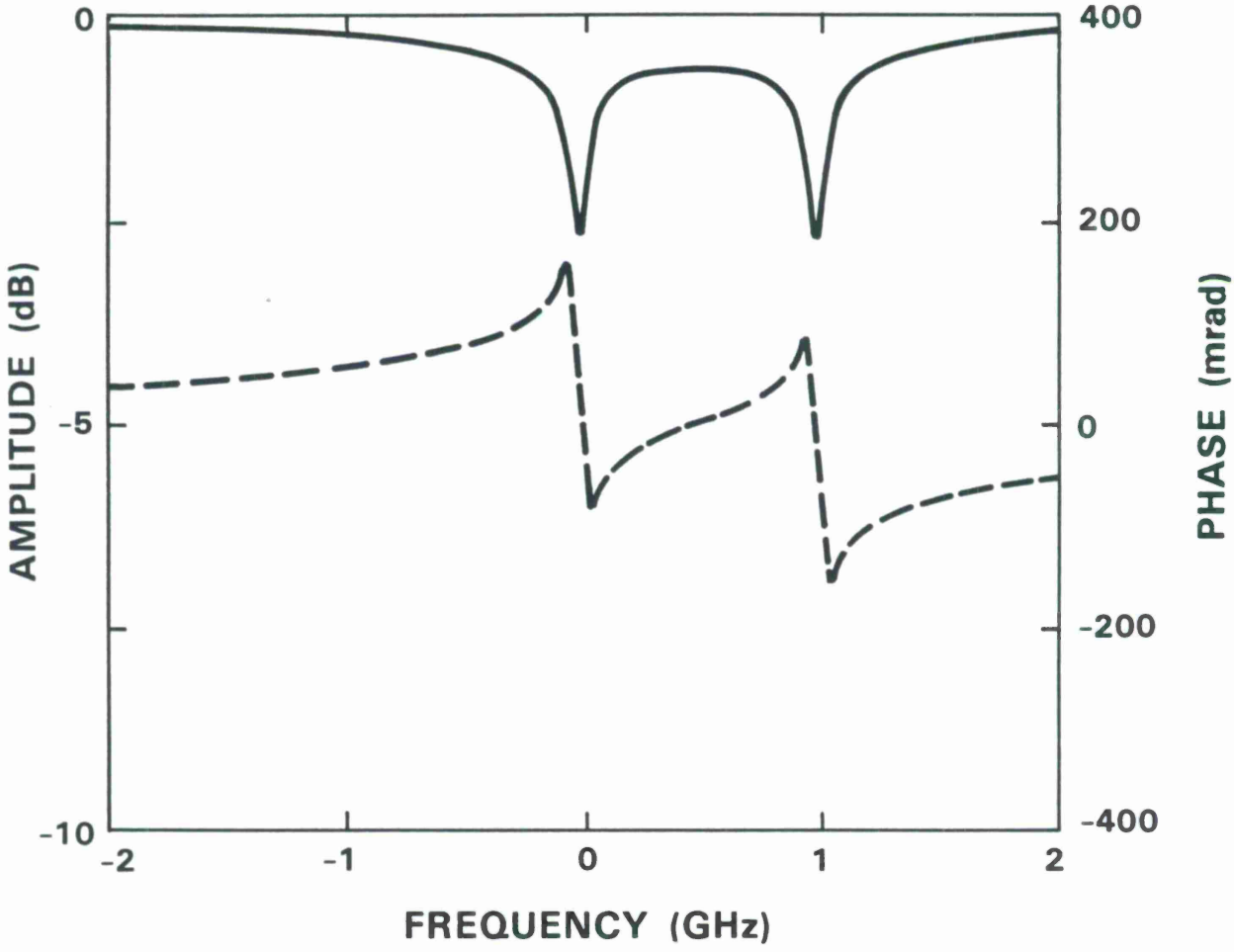

80197-11

Figure 12. Transfer function for a two-way calculation from 10 km, for a 1 GHz target Doppler shift.

$$a(t) = \text{rect}\left(\frac{t}{\Delta t}\right), \tag{17}$$

where

$$\text{rect}(x) = \begin{cases} 1 \; ; & |x| < 0.5 \\ 0 \; ; & |x| > 0.5 \end{cases} \tag{18}$$

The pulse may be compressed by matched filtering (taking its cross-correlation with a reference chirp that is the complex conjugate of the chirp itself). The squared modulus of the correlation is

$$c(t) = \left(\frac{\Delta t - |t|}{\Delta t}\right)^2 \text{sinc}^2\left[(\Delta t - |t|)\left(\frac{B}{\Delta t}\right)t\right] \tag{19}$$

for ($|t| \leq \Delta t$; zero elsewhere) where

$$\text{sinc}(x) = \frac{\sin(\pi x)}{\pi x} \tag{20}$$

For large time bandwidth products ($B\,\Delta t >> 1$) note that Equation 19 can be well approximated for small times ($|t| << \Delta t$) by

$$c(t) \approx \text{sinc}^2(Bt) \tag{21}$$

The first time (corresponding to target range) sidelobe for the sinc - squared function is 13.5 dB (0.045) below the central maximum. Hamming weighting (c.f. Rihaczek [7]) will be used to reduce the range sidelobes (with some loss of resolution) throughout the remainder of this discussion. The form of the weighting is:

$$W(\nu) = \text{rect}\left(\frac{\nu - \nu_0}{B}\right)\left\{0.54 + 0.46\cos\left[\frac{2\pi(\nu - \nu_0)}{B}\right]\right\} \tag{22}$$

5. RANGE SIDELOBES

The target matched filter response may be expressed as

$$p(t) = \left| F.T.^{-1} \{ U_{LFM}(\nu)\, U_R^*(\nu)\, W(\nu)\, T(\nu) \} \right|^2 \qquad (23)$$

where ($F.T.^{-1}$) indicates inverse Fourier transform, U_{LFM} is the Fourier transform of the transmitted chirp, U_R is the transform of the reference chirp (* indicates complex conjugate), W is the weighting function, and T is the two-way atmospheric transfer function.

Figures 13 - 16 show the matched filter responses for the atmospheric absorption of Figure 3 (along a path to space from sea level) for chirp bandwidths of 200 Mhz, 500 MHz, 1 Ghz, and 2 GHz, and a Doppler shift from the target of 1 GHz (transfer function of Figure 11). Figures 17 - 20 are similar curves given a radar at 10 km altitude (atmosphere of Figure 4, transfer function of Figure 12). In Figures 13 - 20 the curves are each shown with a reference Hamming weighted impulse response for comparison.

6. USE OF ISOTOPIC CO_2 LASERS

To avoid both the absorption and dispersion associated with atmospheric CO_2, a radar can be operated on a transition of a different isotopic combination. Ordinary $^{12}C^{16}O_2$ is , which is represented in brief notation (Reference 5) as 626. The isotope combination 636($^{13}C^{16}O_2$) is rare in the atmosphere. Figure 21 shows data from Reference 6 over a spectral region containing two of the strongest lines of this isotope combination. The spectrum is at a resolution of approximately 5×10^{-3} cm^{-1}, and is through less than 2 air masses. Note that the absorption due to naturally occuring $^{13}C^{16}O_2$ is very small, and that there are no accidental overlaps with absorption features due to other species.

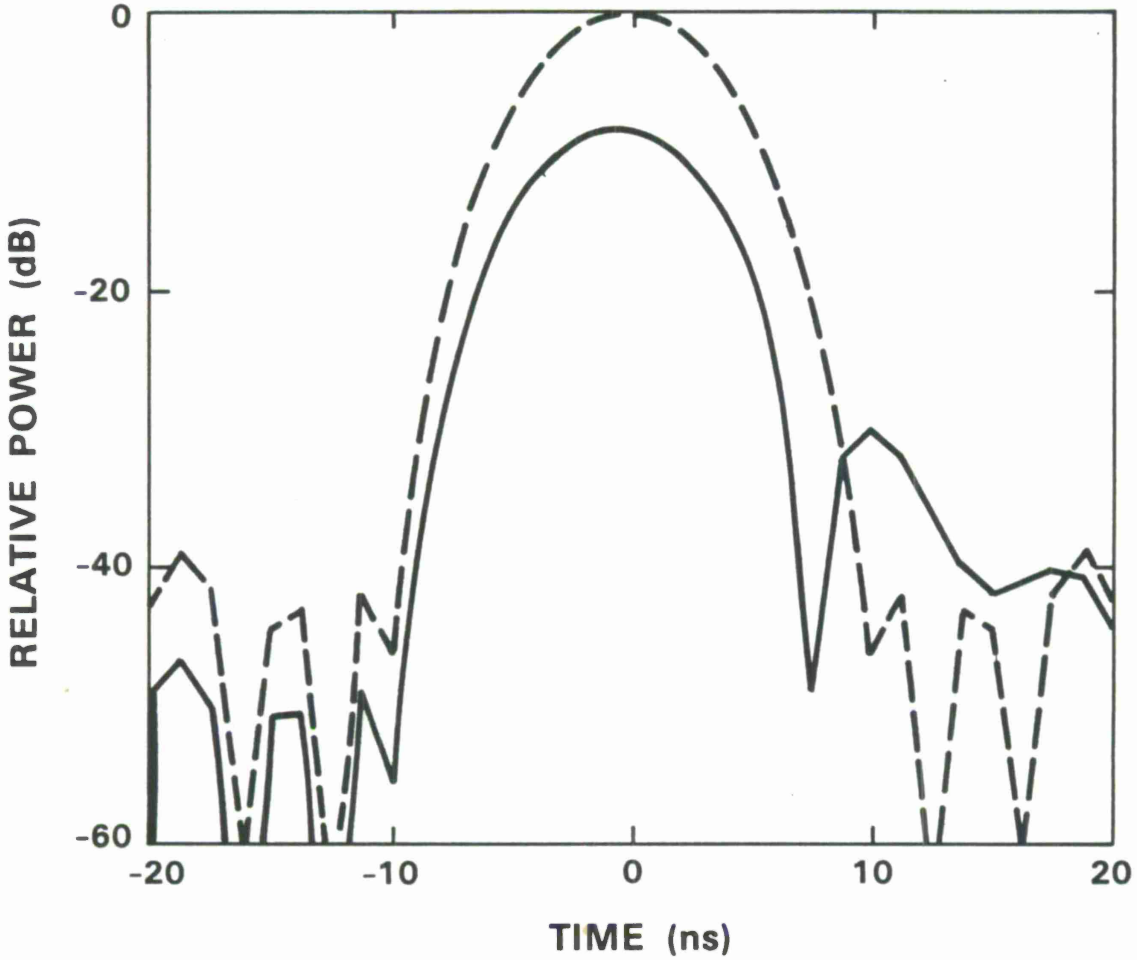

80197-16

Figure 13. Matched filter response for a linear FM chirp pulse with a 200 MHz bandwidth, for the two-way transfer function from sea level.

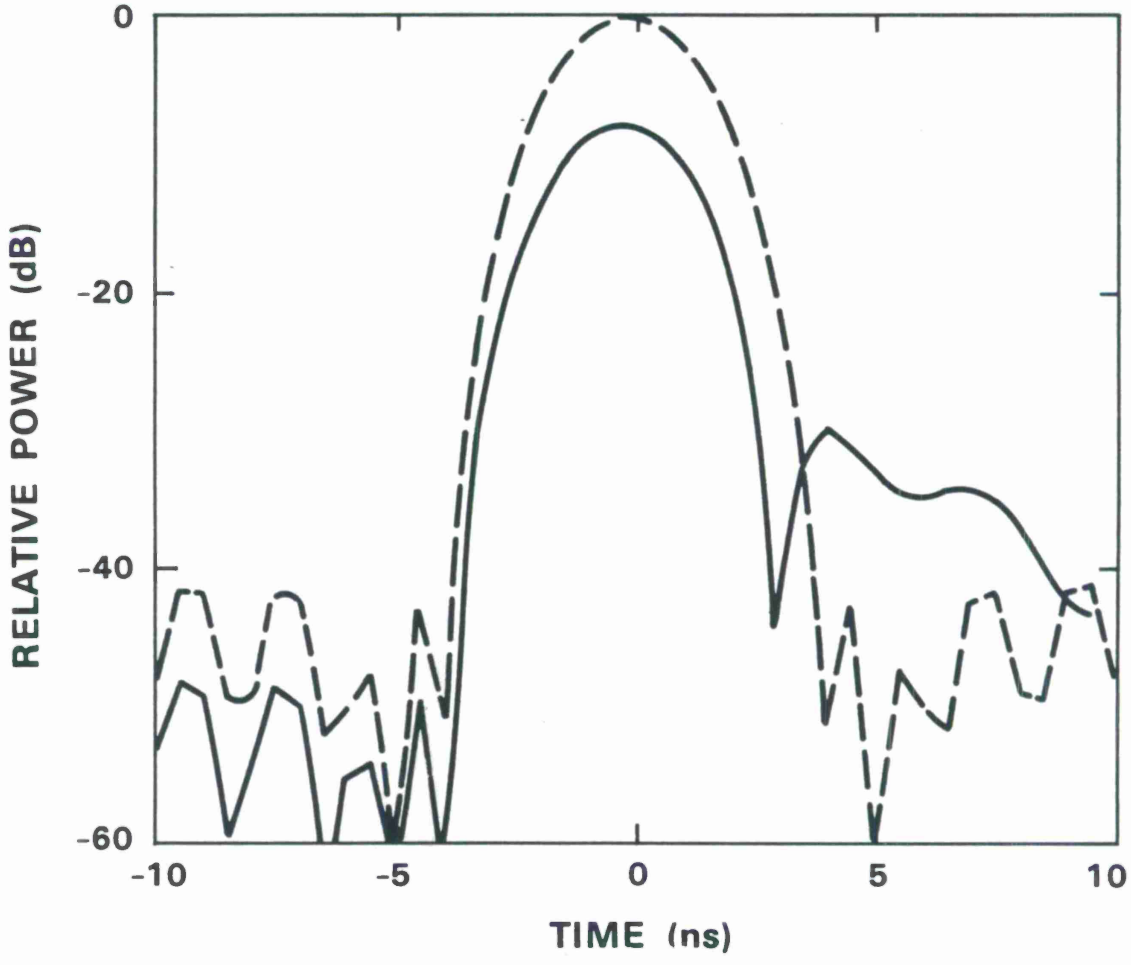

80197-17

Figure 14. Matched filter response, 500 MHz bandwidth, from sea level.

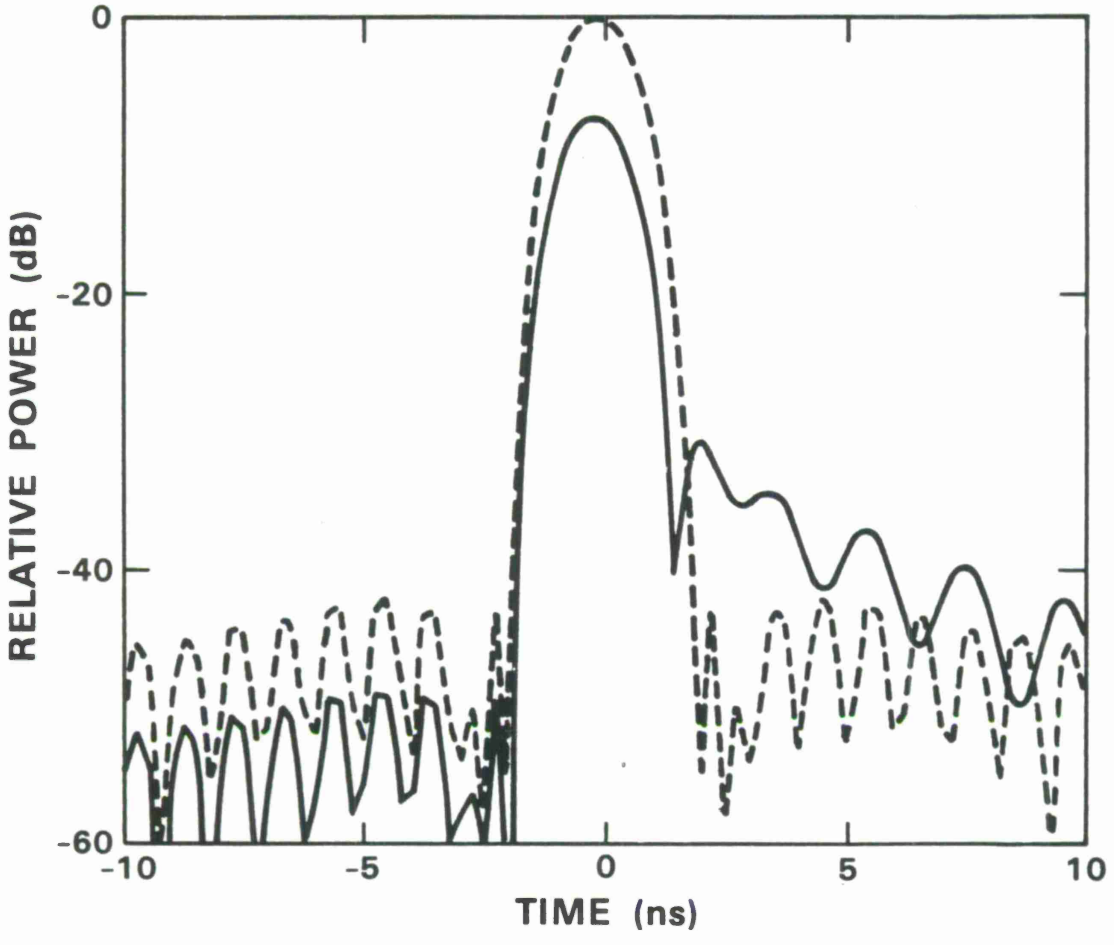

80197-18

Figure 15. Matched filter response, 1 GHz bandwidth, from sea level.

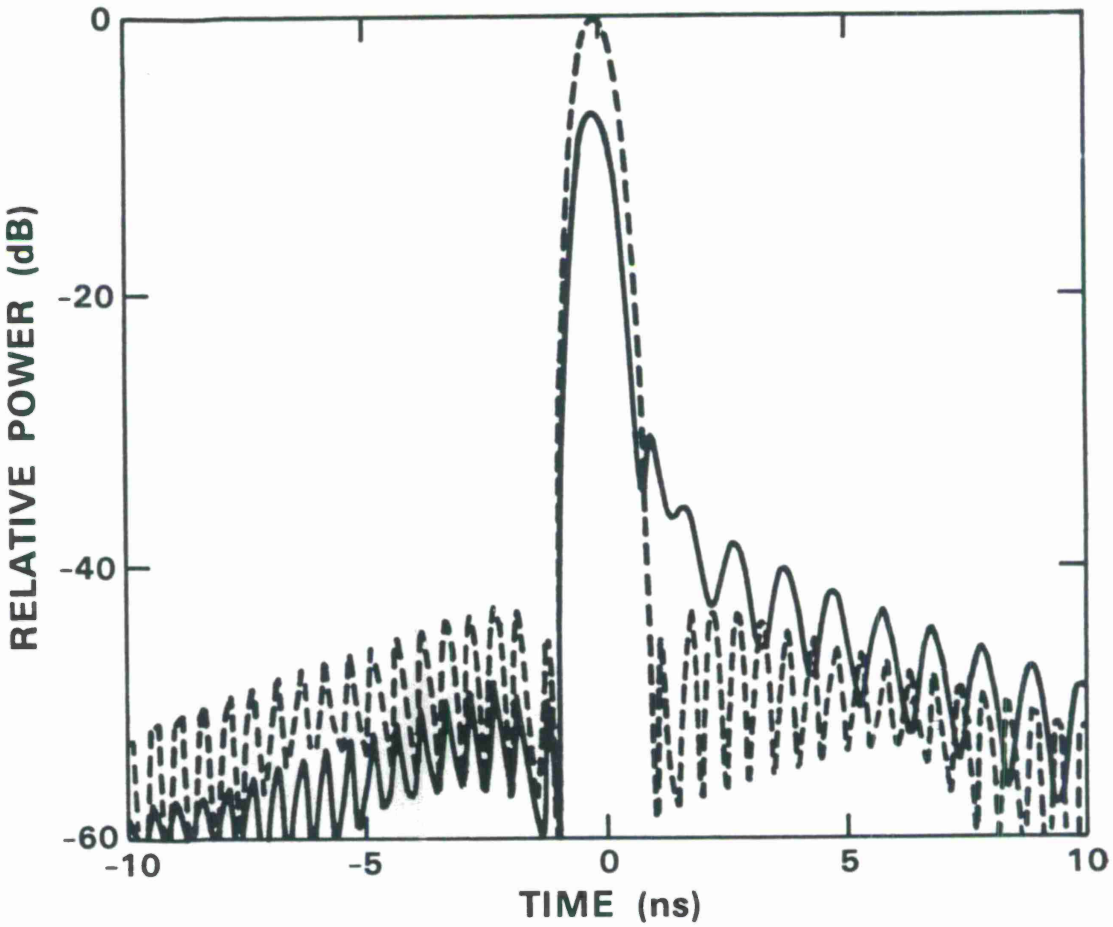

80197-19

Figure 16. Matched filter response, 2 GHz bandwidth, from sea level.

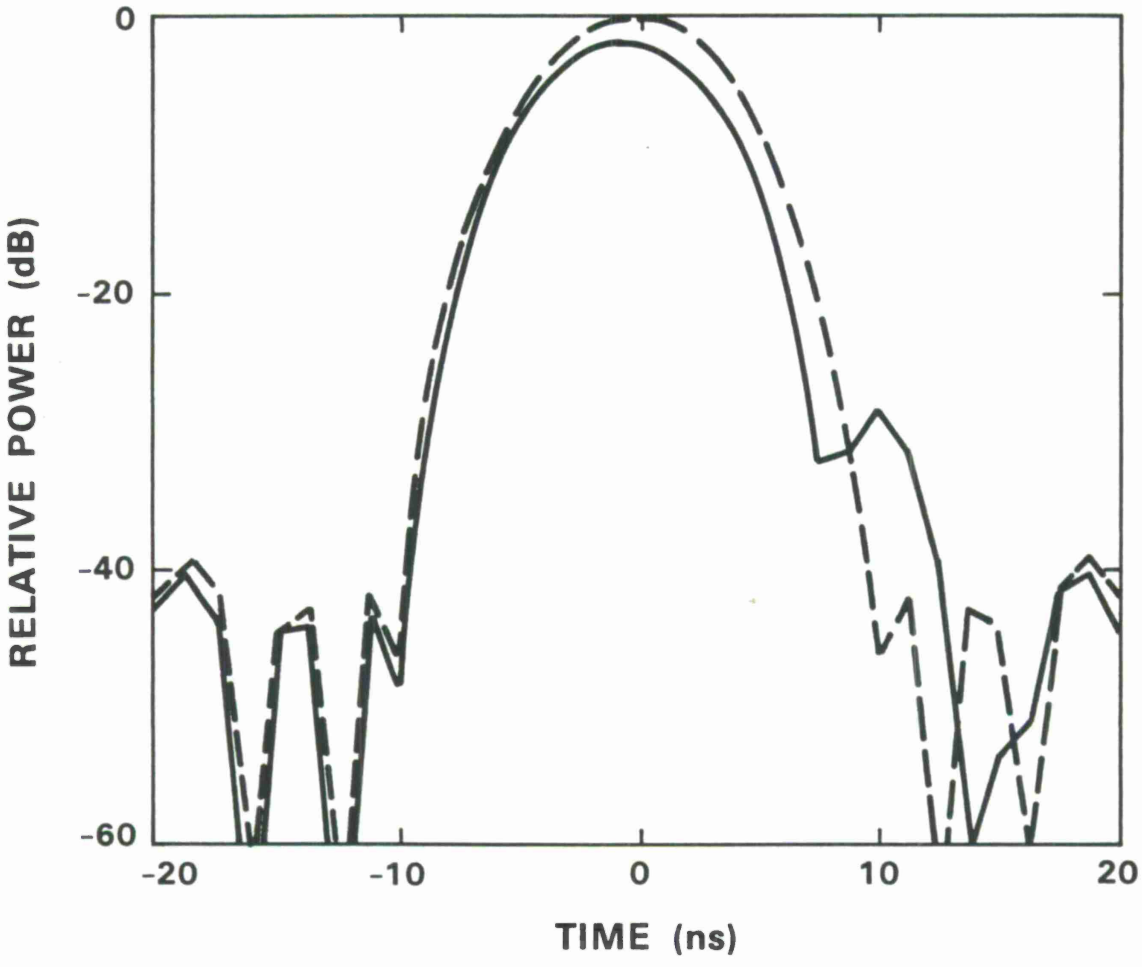

80197-20

Figure 17. Matched filter response for a linear FM chirp pulse with a 200 MHz bandwidth, from 10 km (two-way).

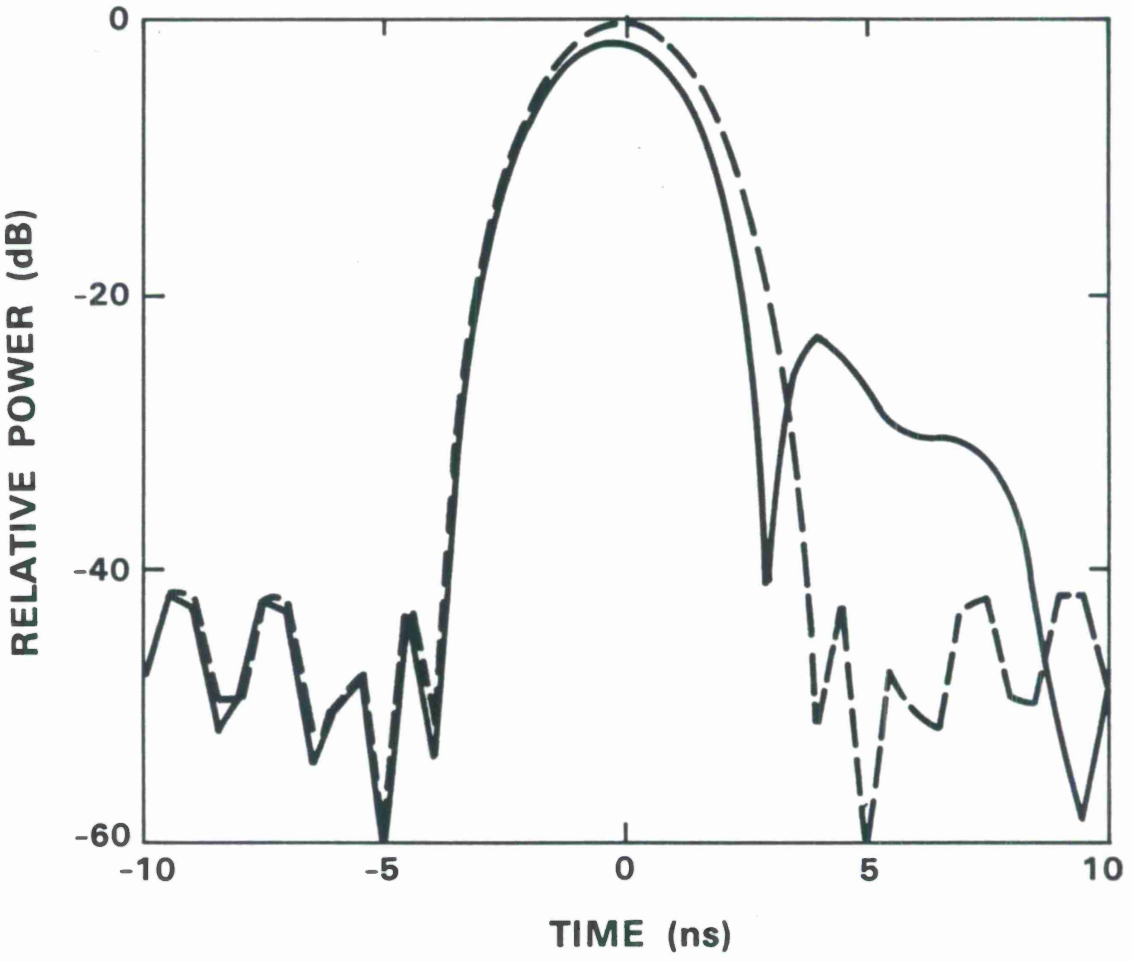

80197-21

Figure 18. Matched filter response, 500 MHz bandwidth, from 10 km.

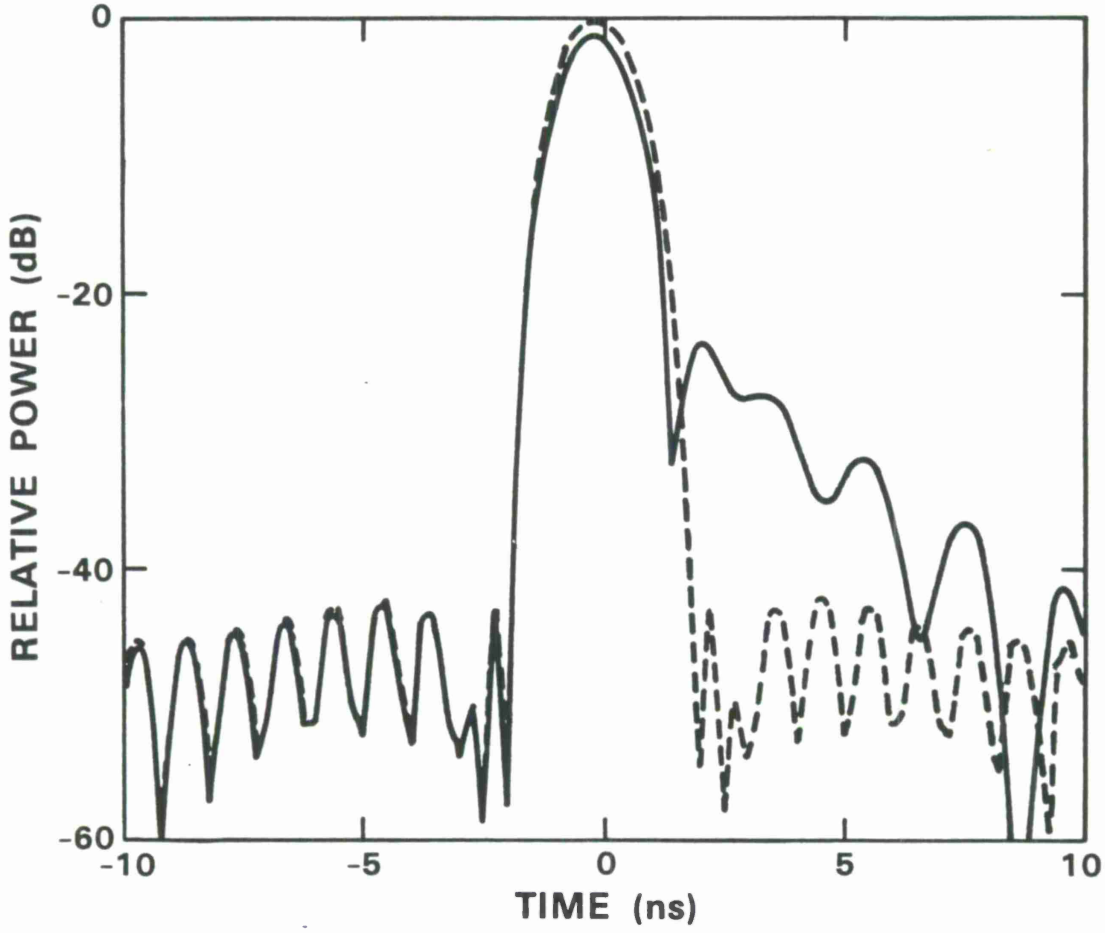

80197-22

Figure 19. Matched filter response, 1 GHz bandwidth, from 10 km.

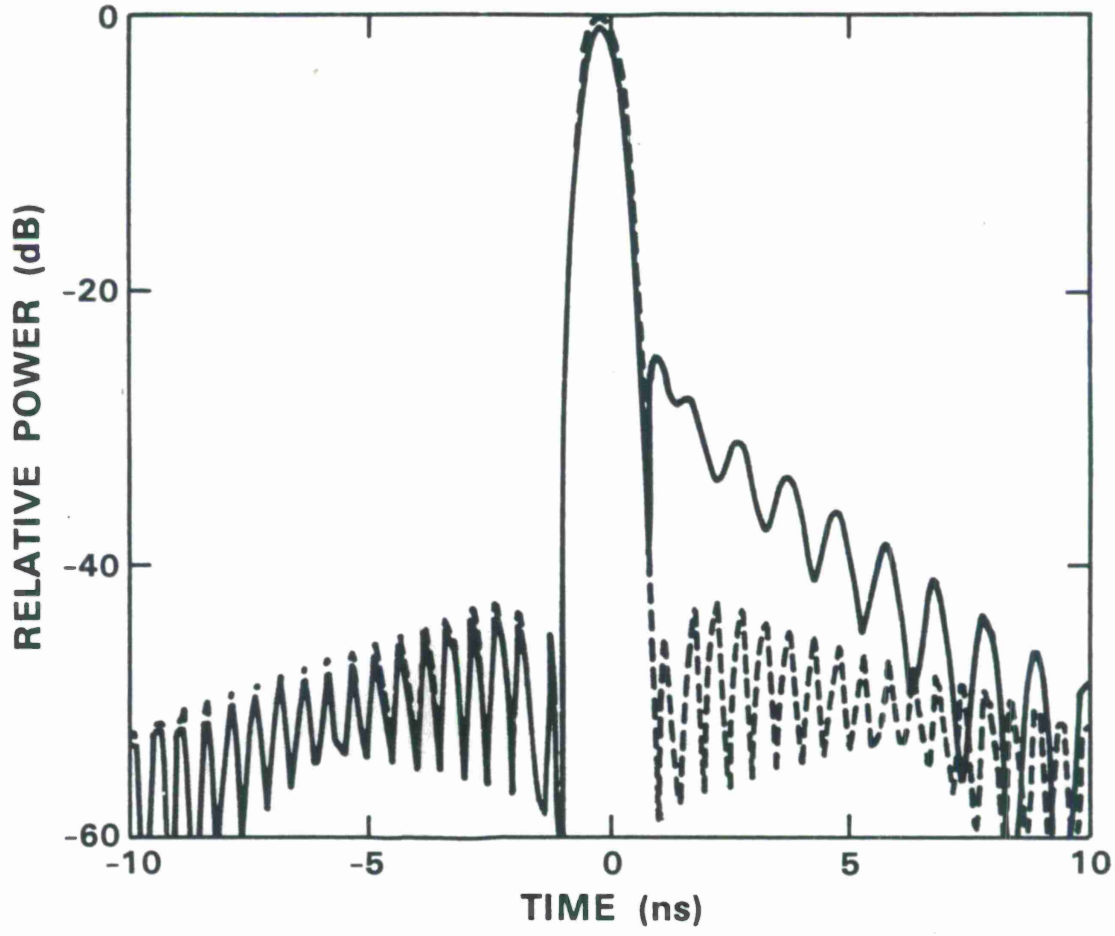

80197-23

Figure 20. Matched filter response, 2 GHz bandwidth, from 10 km.

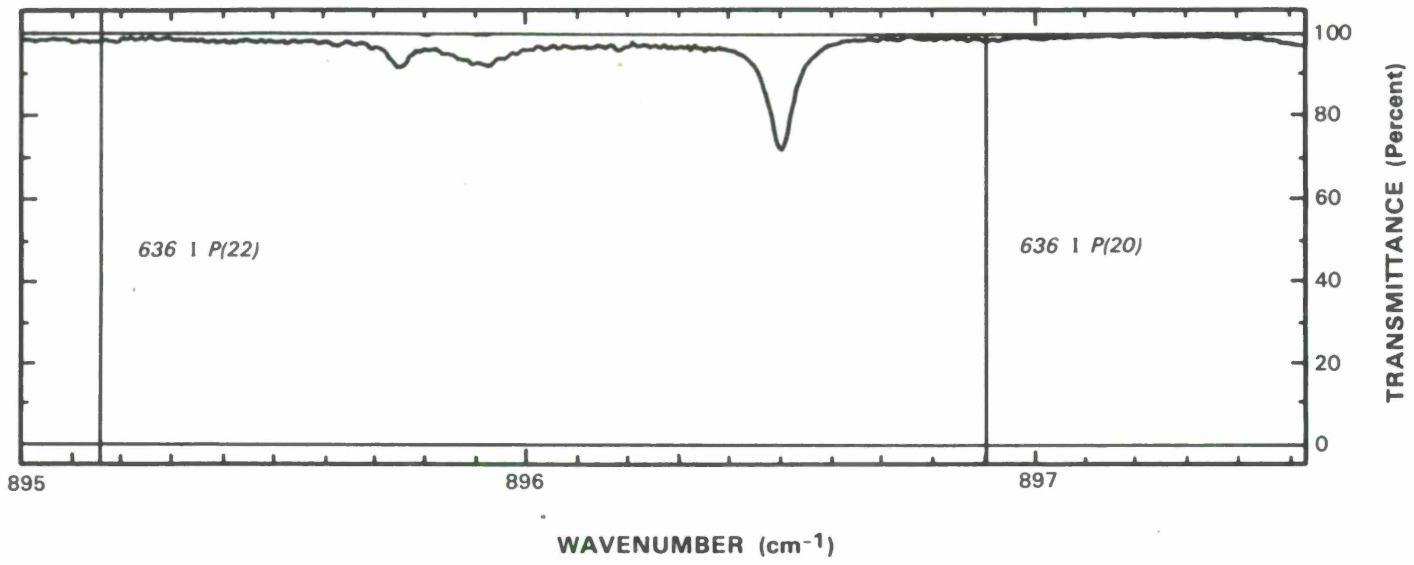

Figure 21. Section of solar absorption spectrum showing transmittance of $^{13}C^{16}O_2$ laser energy.

7. CONCLUSIONS

We have shown that the atmospheric dispersion effects on high-resolution CO_2 laser radars are significant beyond the simple loss of power due to the associated absorption. The principal effect is to increase the range sidelobes of the radar to levels that may be unacceptable for some applications. Range resolution is also degraded, but this effect is small. The calculation on a path from a 10 km altitude shows that the dispersion effects cannot be reduced to low levels by operating a CO_2 laser radar from an aircraft, although the atmospheric transmittance will be notably improved.

Similar effects would apply to any CO_2 laser radar operating with a resolution (bandwidth) comparable to any of those in the above calculations. These would include systems that obtain high range resolution by using short pulses (0.5 - 5 ns duration) or phase coding schemes.

The strongest lasing transitions of ordinary CO_2 appear to be poor choices for operation through the atmosphere. Other transitions that would be weakly absorbed, especially those of rarer isotope combinations (e.g., $^{13}C^{16}O_2$, $^{13}C^{18}O_2$), will be preferred.

ACKNOWLEDGEMENTS

The authors wish to thank L. Bradley and C. Buczek for their advice, and to thank E. B. Craig for performing the FASCOD2 calculations.

REFERENCES

1. J. J. P. Smith, D. J. Dube, M. E. Gardner, S. A. Clough, F. X. Kneizys, and L. S. Rothman, *FASCODE - Fast Atmospheric Signature Code (Spectral Transmittance and Radiance)* , Air Force Geophysics Laboratory, AF - TR - 78 - 0081, 1978, ADA-057506.

2. W. H. Hallidy, *Dispersive Propagation of a Chirped Pulse* , to be published in the Proceedings of the Fifth International Conference on Antennas and Propagation, York, England, 30 March - 2 April 1987.

3. A. Yariv, *Quantum Electronics* , Second Edition, John Wiley & Sons, New York, 1975.

4. R. N. Bracewell, *The Fourier Transform and its Applications* , Second Edition, McGraw - Hill, New York, 1978.

5. L. C. Bradley, K. L. Soohoo, and C. Freed, *Absolute Frequencies of Lasing Transitions in Nine CO_2 Isotopic Species* , IEEE Journal of Quantum Electronics, Vol. QE-22, No. 2, Feb. 1986, pp. 234-267.

6. J. Brault, National Solar Observatory, P. O. Box 26732, Tucson, AZ 85726, private communication.

7. A. Rihaczek, *Principles of High Resolution Radar* , Peninsula Publishing, Los Altos, CA 1985.

REPORT DOCUMENTATION PAGE

1a. REPORT SECURITY CLASSIFICATION Unclassified	1b. RESTRICTIVE MARKINGS
2a. SECURITY CLASSIFICATION AUTHORITY	3. DISTRIBUTION/AVAILABILITY OF REPORT Approved for public release; distribution is unlimited.
2b. DECLASSIFICATION/DOWNGRADING SCHEDULE	
4. PERFORMING ORGANIZATION REPORT NUMBER(S) ODT-8	5. MONITORING ORGANIZATION REPORT NUMBER(S) ESD-TR-87-084
6a. NAME OF PERFORMING ORGANIZATION Lincoln Laboratory, MIT 6b. OFFICE SYMBOL *(If applicable)*	7a. NAME OF MONITORING ORGANIZATION Electronic Systems Division
6c. ADDRESS *(City, State, and Zip Code)* P.O. Box 73 Lexington, MA 02173-0073	7b. ADDRESS *(City, State, and Zip Code)* Hanscom AFB, MA 01731
8a. NAME OF FUNDING/SPONSORING ORGANIZATION Defense Advanced Research Projects Agency 8b. OFFICE SYMBOL *(If applicable)*	9. PROCUREMENT INSTRUMENT IDENTIFICATION NUMBER F19628-85-C-0002
8c. ADDRESS *(City, State, and Zip Code)* 1400 Wilson Boulevard Arlington, VA 22209	10. SOURCE OF FUNDING NUMBERS PROGRAM ELEMENT NO. 63220C; PROJECT NO. 309; TASK NO. 3391; WORK UNIT ACCESSION NO.
11. TITLE *(Include Security Classification)* Distortion of Wideband Carbon Dioxide Laser Radar Waveforms due to Atmospheric Dispersion and Absorption	
12. PERSONAL AUTHOR(S) Robert E. Knowlden, Alan L. Kachelmyer, and William E. Keicher	
13a. TYPE OF REPORT Project Report 13b. TIME COVERED FROM _____ TO _____	14. DATE OF REPORT *(Year, Month, Day)* 12 November 1987 15. PAGE COUNT 42
16. SUPPLEMENTARY NOTATION None	

17. COSATI CODES			18. SUBJECT TERMS *(Continue on reverse if necessary and identify by block number)*
FIELD	GROUP	SUB-GROUP	laser radar ladar atmospheric dispersion

19. ABSTRACT *(Continue on reverse if necessary and identify by block number)*

Atmospheric dispersion is shown to have a significant effect on wideband coherent laser radars operating on a transition of ordinary carbon dioxide (CO_2). Calculations are performed for a hypothetical ground-based laser radar that is observing targets in low Earth orbit. Linear frequency modulated (LFM) waveforms of bandwidths 200 MHz, 500 MHz, 1 GHz, and 2 GHz are used. The use of a laser radar operating with a different carbon isotope ($^{13}C^{16}O_2$) is suggested to avoid the dispersion problem, and also to reduce the atmospheric absorption.

20. DISTRIBUTION/AVAILABILITY OF ABSTRACT ☐ UNCLASSIFIED/UNLIMITED ☒ SAME AS RPT. ☐ DTIC USERS	21. ABSTRACT SECURITY CLASSIFICATION Unclassified
22a. NAME OF RESPONSIBLE INDIVIDUAL Lt. Col. Hugh L. Southall, USAF	22b. TELEPHONE *(Include Area Code)* (617) 863-5500, Ext. 2330 22c. OFFICE SYMBOL ESD/TML